SUPPLEMENTARY INFORMATION

Comparison of microfluidic digital PCR and conventional quantitative PCR for measuring copy number variation.

Alexandra S Whale[1], Jim Huggett[1]*, Simon Cowen[1], Valerie Speirs[2], Rebecca Sanders[1], Jacqui Shaw[3] Stephen Ellison[1], Carole A Foy[1] and Daniel J Scott[1]

[1] Molecular and Cell Biology, LGC Limited, Queens Road, Teddington, Middlesex TW11 0LY

[2] Leeds Institute of Molecular Medicine, University of Leeds, St James's University Hospital, Leeds LS9 7TF UK

[3] Cancer Studies & Molecular Medicine, University of Leicester, Robert Kilpatrick Clinical Sciences Building, PO Box 65 Leicester Royal Infirmary, Leicester LE2 7LX

*Corresponding author

Contents:

Supplementary Table 1. MIQE checklist for authors, reviewers and editors.

ITEM TO CHECK	IMPORTANCE	CHECKLIST	COMMENTS/ WHERE?
EXPERIMENTAL DESIGN			
Definition of experimental and control groups	**E**	**YES**	Materials and Methods
Number within each group	**E**	**YES**	Materials and Methods
Assay carried out by core lab or investigator's lab?	D	**YES**	Investigators lab
Acknowledgement of authors' contributions	D	**NO**	Not required by journal
SAMPLE			
Description	**E**	**N/A**	
Volume/mass of sample processed	D	**N/A**	
Microdissection or macrodissection	**E**	**N/A**	
Processing procedure	**E**	**N/A**	
If frozen - how and how quickly?	**E**	**N/A**	
If fixed - with what, how quickly?	**E**	**N/A**	
Sample storage conditions and duration (especially for FFPE samples)	**E**	**N/A**	
NUCLEIC ACID EXTRACTION			
Procedure and/or instrumentation	**E**	**N/A**	All gDNA was purchased. Part numbers and maufactures are given in Materials and Methods
Name of kit and details of any modifications	**E**	**N/A**	
Source of additional reagents used	D	**N/A**	
Details of DNase or RNAse treatment	**E**	**N/A**	
Contamination assessment (DNA or RNA)	**E**	**N/A**	
Nucleic acid quantification	**E**	**YES**	Materials and Methods
Instrument and method	**E**	**YES**	Materials and Methods
Purity (A260/A280)	D	**YES**	Materials and Methods
Yield	D	**N/A**	
RNA integrity method/instrument	**E**	**N/A**	
RIN/RQI or Cq of 3' and 5' transcripts	**E**	**N/A**	
Electrophoresis traces	D	**N/A**	
Inhibition testing (Cq dilutions, spike or other)	**E**	**YES**	Sup. Figure 1
REVERSE TRANSCRIPTION			
Complete reaction conditions	**E**	**N/A**	
Amount of RNA and reaction volume	**E**	**N/A**	
Priming oligonucleotide (if using GSP) and concentration	**E**	**N/A**	
Reverse transcriptase and concentration	**E**	**N/A**	
Temperature and time	**E**	**N/A**	
Manufacturer of reagents and catalogue numbers	D	**N/A**	
Cqs with and without RT	D*	**N/A**	
Storage conditions of cDNA	D	**N/A**	

qPCR TARGET INFORMATION			
Sequence accession number	**E**	**YES**	HER2: NG_007503, RNaseP: NR_002312.1
Location of amplicon	D	**YES**	Materials and Methods
Amplicon length	**E**	**YES**	Sup. Figure 1
In silico specificity screen (BLAST, etc)	**E**	**YES**	Sup. Figure 1
Pseudogenes, retropseudogenes or other homologs?	D	**YES**	None detected by BLASTn
Sequence alignment	D	**YES**	Sup. Figure 1
Secondary structure analysis of amplicon	D	**N/A**	
Location of each primer by exon or intron (if applicable)	**E**	**YES**	Materials and Methods & Sup. Figure 1
What splice variants are targeted?	**E**	**N/A**	
qPCR OLIGONUCLEOTIDES			
Primer sequences	**E**	**YES**	Materials and Methods (1)
RTPrimerDB Identification Number	D	**N/A**	
Probe sequences	D**	**YES**	Materials and Methods (1)
Location and identity of any modifications	**E**	**N/A**	
Manufacturer of oligonucleotides	D	**YES**	Materials and Methods
Purification method	D	**YES**	HPLC
qPCR PROTOCOL			
Complete reaction conditions	**E**	**YES**	Materials and Methods
Reaction volume and amount of cDNA/DNA	**E**	**YES**	Materials and Methods
Primer, (probe), Mg++ and dNTP concentrations	**E**	**YES**	Materials and Methods; Manufactures proprietary
Polymerase identity and concentration	**E**	**YES**	AmpliTaq Gold® DNA Polymerase, UP (Ultra Pure)
Buffer/kit identity and manufacturer	**E**	**YES**	Materials and Methods
Exact chemical constitution of the buffer	D	**NO**	Manufactures proprietary
Additives (SYBR Green I, DMSO, etc.)	**E**	**N/A**	
Manufacturer of plates/tubes and catalog number	D	**YES**	ABI 96-well plates (4306737)
Complete thermocycling parameters	**E**	**YES**	Materials and Methods
Reaction setup (manual/robotic)	D	**YES**	Manual setup
Manufacturer of qPCR instrument	**E**	**YES**	Materials and Methods
qPCR VALIDATION			
Evidence of optimisation (from gradients)	D	**YES**	Standard curve quantification: Sup. Figure 1
Specificity (gel, sequence, melt, or digest)	**E**	**NO**	Not possible after digital PCR
For SYBR Green I, Cq of the NTC	**E**	**N/A**	
Standard curves with slope and y-intercept	**E**	**YES**	Sup. Figure 1

PCR efficiency calculated from slope	**E**	**YES**	Sup. Figure 1
Confidence interval for PCR efficiency or standard error	D	**N/A**	
R2 of standard curve	**E**	**YES**	Sup. Figure 1
Linear dynamic range	**E**	**YES**	Sup. Figure 1
Cq variation at lower limit	**E**	**YES**	Sup. Figure 1
Confidence intervals throughout range	D	**YES**	Figures 1, 2 & 3
Evidence for limit of detection	**E**	**YES**	Figure 2
If multiplex, efficiency and LOD of each assay.	**E**	**YES**	No multiplex assays
DATA ANALYSIS			
qPCR analysis program (source, version)	**E**	**YES**	Materials and Methods
Cq method determination	**E**	**YES**	Materials and Methods
Outlier identification and disposition	**E**	**YES**	Materials and Methods
Results of NTCs	**E**	**YES**	Materials and Methods, Figure 1, Sup. Figure 1, Sup. Figure 2
Justification of number and choice of reference genes	**E**	**N/A**	
Description of normalisation method	**E**	**YES**	Standard curve quantification
Number and concordance of biological replicates	D	**N/A**	
Number and stage (RT or qPCR) of technical replicates	**E**	**YES**	Materials and Methods
Repeatability (intra-assay variation)	**E**	**YES**	Materials and Methods
Reproducibility (inter-assay variation, %CV)	D	**NO**	
Power analysis	D	**YES**	Figure 3
Statistical methods for result significance	**E**	**YES**	Materials and Methods
Software (source, version)	**E**	**YES**	Materials and Methods
Cq or raw data submission using RDML	D	**N/A**	

All essential information (E) must be submitted with the manuscript. Desirable information (D) should be submitted if available. If using primers obtained from RTPrimerDB, information on qPCR target, oligonucleotides, protocols and validation is available from that source.

(1) Primer and probe sequences for HER2 assays included in material and methods, RNaseP primer and probe sequences are not disclosed by provider, but amplicon sequence is given in Supplementary Figure 1

*: Assessing the absence of DNA using a no RT assay is essential when first extracting RNA. Once the sample has been validated as RDNA-free, inclusion of a no-RT control is desirable, but no longer essential.

**: Disclosure of the probe sequence is highly desirable and strongly encouraged. However, since not all commercial pre-designed assay vendors provide this information, it cannot be an essential requirement. Use of such assays is advised against.

Supplementary Table 2. Generation of *in vitro* HER2 gene amplification model

% Normal female gDNA	% T-47D gDNA	Expected HER2:RNaseP
100	0	1.03
90	10	1.12
85	15	1.17
80	20	1.22
75	25	1.27
70	30	1.32
50	50	1.51
0	100	2.00

Expected HER2:RNaseP ratios are calculated from the dPCR experimental values obtained for 100% normal female gDNA (1.03) and 100% T-47D gDNA (2.00) (Figure 1b) using the equation:

Expected ratio = ((% T-47D gDNA x ratio for 100% T-47D gDNA) + (% Normal female gDNA x ratio for 100% Normal female gDNA)) / 100.

(a)

ref|NR_002312.1| Homo sapiens ribonuclease P RNA component H1 (RPPH1), RNase P RNA (Length=341)

GENE ID: 85495 RPPH1 | ribonuclease P RNA component H1 [Homo sapiens]

```
 Score = 156 bits (84), Expect = 7e-38
 Identities = 87/87 (99%), Gaps = 0/87 (0%)
 Strand=Plus/Plus

Query  1   GCGGAGGGAAGCTCATCAGTGGGGCCACGAGCTGAGTGCGTCCTGTCACTCCACTCCCAT  60
           ||||||||||||||||||||||||||||||||||||||||||||||||||||||||||||
Sbjct  6   GCGGAGGGAAGCTCATCAGTGGGGCCACGAGCTGAGTGCGTCCTGTCACTCCACTCCCAT  65

Query  61  GTCCCTTGGGAAGGTCTGAGACTAGGG  87
           |||||||||||||||||||||||||||
Sbjct  66  GTCCCTTGGGAAGGTCTGAGACTAGGG  92
```

(b)

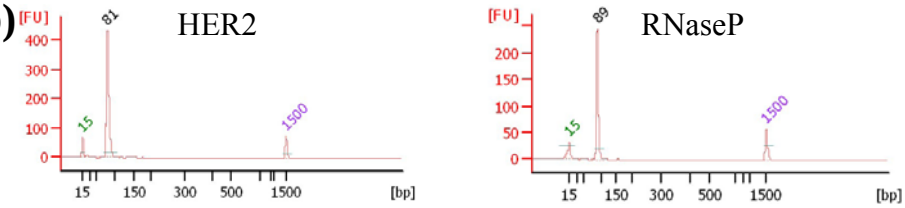

(c)

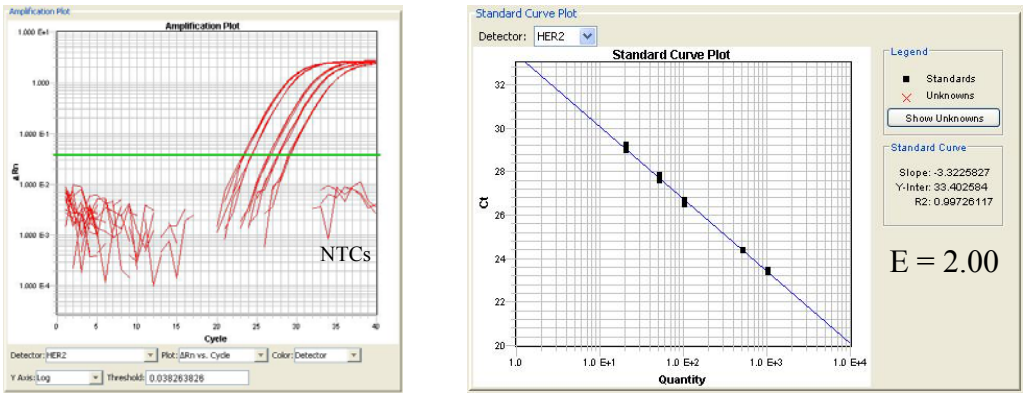

(d)

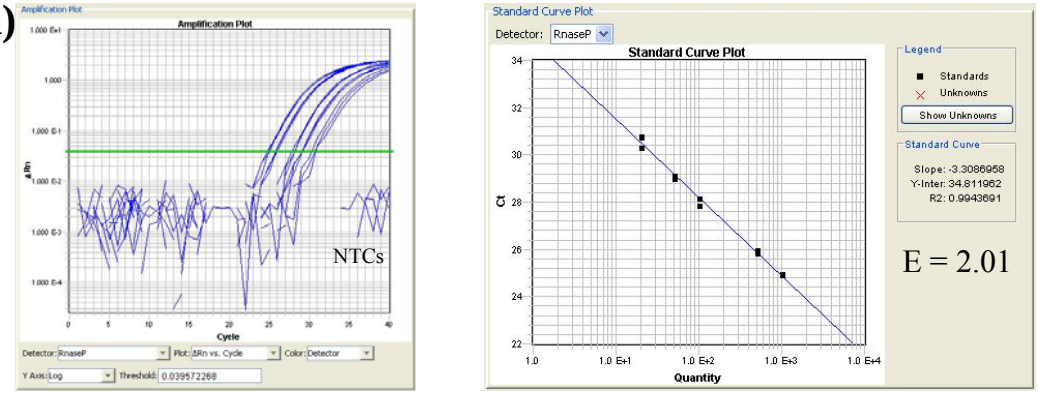

Supplementary Figure 1. Assay performance for real-time quantitative PCR in accordance with the MIQE guidelines. (a) Alignment of RNaseP amplicon following clonal sequencing with NR_002312.1 using BLASTn. (b) 2100 Bioanalyzer traces confirming amplification of a single PCR product for HER2 and RNaseP assays. (c-d) SDS v2.4 software generated amplification plots and standard curves for (c) HER2 and (d) RNaseP assays used to generate data for Figure 2. PCR efficiency (E) is calculated from the slope of the standard curve for both assays where PCR efficiency = $10^{(-1/\text{slope})}$. NTC amplification curves are shown for both HER2 and RNaseP assays demonstrating no amplification.

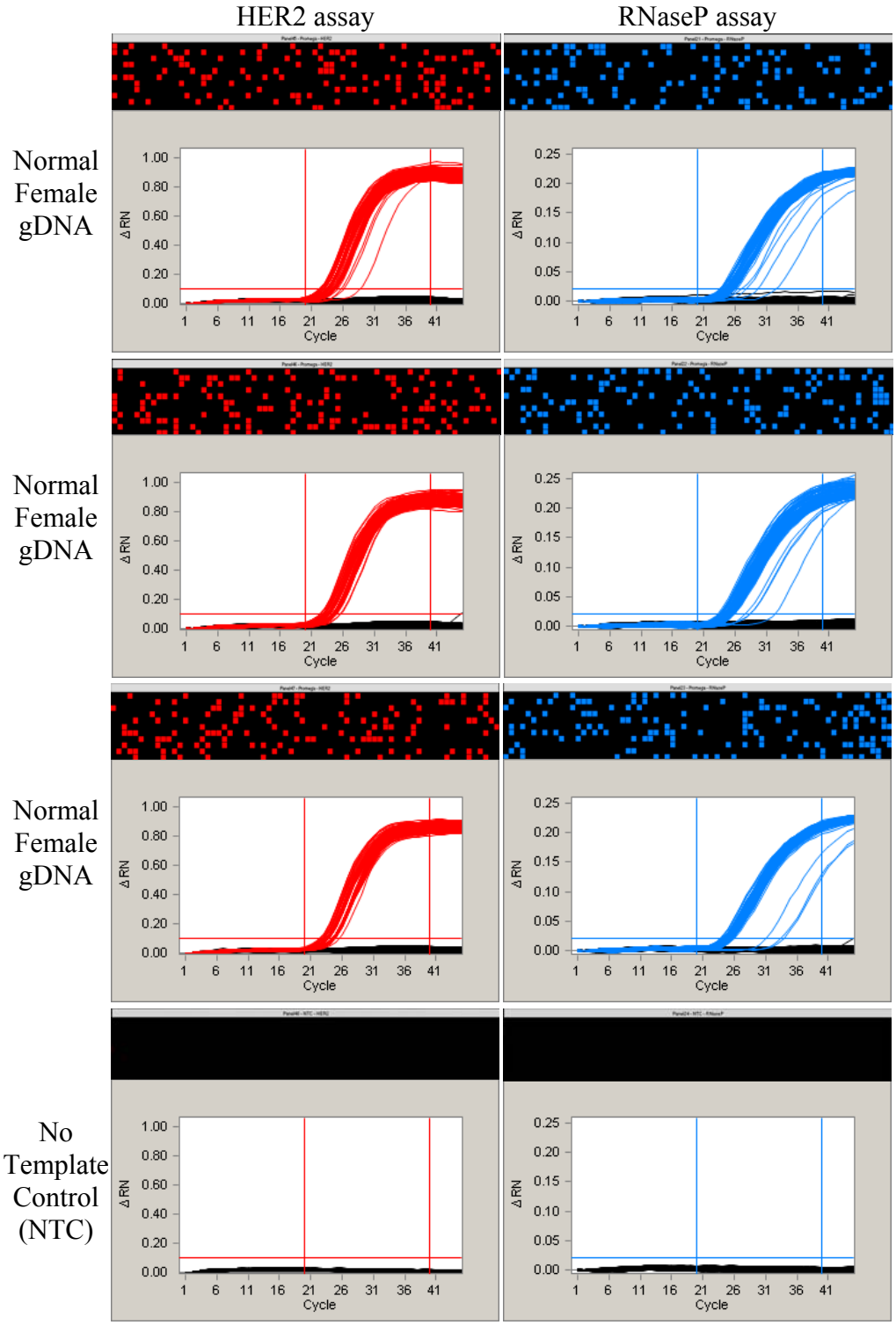

Supplementary Figure 2. Assay performance for digital PCR. Digital PCR Analysis software generated heat maps and amplification curves for triplicate panels for HER2 and RNaseP assays on normal female gDNA. Each panel contains a total of 770 chambers that have either positive (HER2; red and RNaseP; blue) or negative (black) amplification signals. Amplification curves for each panel are show underneath their respective heat maps demonstrating the spread of amplification curves for each panel. The corresponding heat maps and amplification curves for the NTC panels show that no amplification occurs in any chambers. Horizontal lines in the amplification plots represent the Cq threshold while the two vertical lines represent the Cq target range.

SUPPLEMENTARY STATISTICAL INFORMATION

Estimated variance for the log ratio in digital PCR

Let L_t and L_r be variables representing the observed copy number per chamber for the target and reference samples respectively in a digital PCR experiment with C chambers. The variance of the quantity $R = \ln(L_t/L_r)$ can be estimated for the range of most interest using first order error propagation. This yields

$$\mathrm{var}(R) \approx \frac{\mathrm{var}(L_t)}{E(L_t)^2} + \frac{\mathrm{var}(L_r)}{E(L_r)^2} \tag{S1}$$

where $E(L_t)$ and $E(L_r)$ are the expected values of L_t and L_r. Let $L_i = \ln(1 - H_i/C)$, H_i being the number of positive observations ('hits') on a panel (or group of panels) of size C. Using error propagation as before,

$$\mathrm{var}(L_i) \approx \frac{\mathrm{var}(H_i)}{\left[C(1 - E(H_i)/C)\right]^2} \tag{S2}$$

The variable H_i is binomially distributed, since it consists of the number of positive chambers out of a total number C, and the probability of a positive observation is fixed at $E(H_i)/C = 1 - e^{-E(L_i)}$. The variance of H_i therefore depends on its expected value $E(H_i)$ and the number of chambers C as follows:

$$\mathrm{var}(H_i) = E(H_i)\left[1 - \frac{E(H_i)}{C}\right] \tag{S3}$$

The relation $L_i = \ln(1 - H_i/C)$ between L_i and H_i can be used to rewrite var(R) as

$$\mathrm{var}(R) \approx \frac{Ce^{-E(L_t)}\left(1 - e^{-E(L_t)}\right)}{\left[CE(L_t)e^{-E(L_t)}\right]^2} + \frac{Ce^{-E(L_r)}\left(1 - e^{-E(L_r)}\right)}{\left[CE(L_r)e^{-E(L_t)}\right]^2} = \frac{1 - e^{-E(L_t)}}{CE(L_t)^2 e^{-E(L_t)}} + \frac{1 - e^{-E(L_r)}}{CE(L_r)^2 e^{-E(L_r)}} \tag{S4}$$

This can be rewritten in terms of the true copy numbers per chamber λ_i to give

$$\mathrm{var}(R) \approx \frac{1 - e^{-\lambda_t}}{C\lambda_t^2 e^{-\lambda_t}} + \frac{1 - e^{-\lambda_r}}{C\lambda_r^2 e^{-\lambda_r}} = \frac{1}{C}\left(\frac{e^{\lambda_t} - 1}{\lambda_t^2} + \frac{e^{\lambda_r} - 1}{\lambda_r^2}\right) \tag{S5}$$

When the values for λ_t and λ_r are based on estimates, as they are in most experiments, the variance for the binomial distribution is biased, underestimating var(H_i) by a factor $(C - 1)/C$. In such cases, the C in equation S5 should, strictly speaking, be replaced by $C - 1$, but since C is so large in digital PCR it is not necessary to do this. In our calculations, we have used equation S5 without modification. Equation S5 is given as equation 2 in the manuscript.

To test how well equation S5 fitted the data generated using the underlying Poisson distributions, a simulation consisting of 5,000 replicate experiments, each of two groups of eight 770-chamber panels (a total of 6,160 chambers) was carried out (Supplementary Figure 3a). This corresponded to a fairly typical dPCR experiment operating within its optimum range. The number of molecules in each chamber for the two groups was drawn from two different Poisson distributions: where λ_t has a value of 0.24 and λ_r has a value of 0.20 to give a true copy number ratio of 1.2. The best-fit mean and standard deviation of the log ratio R were 0.1836 and 0.0408 respectively, which

compare well with the values of 0.1823 and 0.0408 predicted using equation S5. The 5,000-point data set passes an Anderson-Darling test for normality ($p = 0.28$), indicating good adherence to a Normal distribution even in the tail area (Supplementary figure 3a).

It would also be useful to compare equation S5 with observed precision for ratios. Unfortunately, while the data available included replication at the individual count level, there was no natural pairing from which the ratios could naturally arise. To obtain a direct estimate of the dispersion of log ratios in a single-panel experiment, we therefore took the standard deviation of log ratios of HER2 and RNaseP observations paired randomly from within each treatment group (Supplementary Figure 3b). Comparison of the observed standard deviation of R with the theoretical standard deviation estimated using equation S5 demonstrated that the experimental data fitted well with the theory (Supplementary Figure 3b).

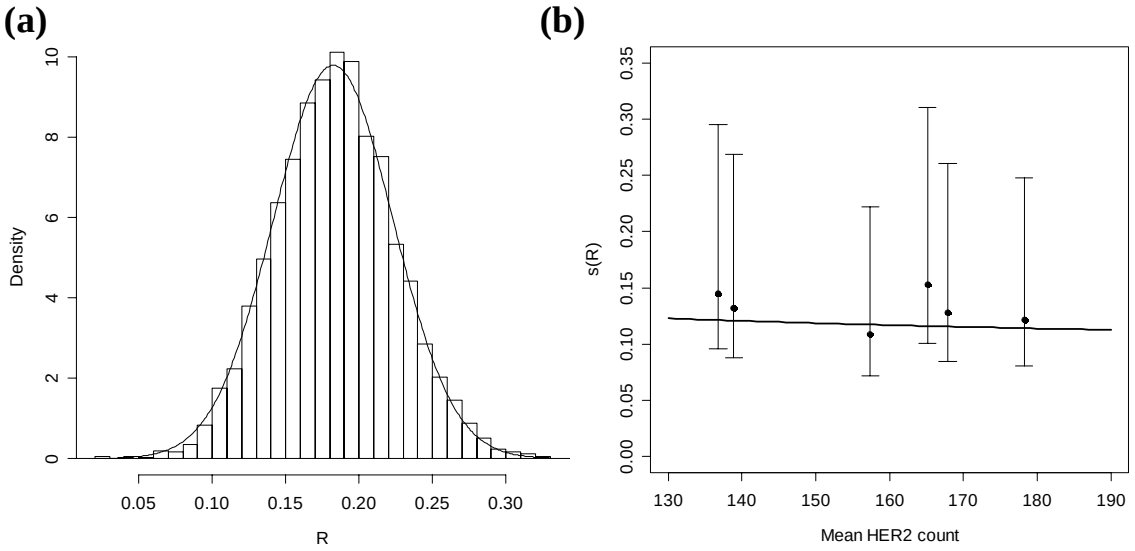

Supplementary Figure 3. Characterisation of the log ratio for a typical dPCR experiment. (a) Distribution of the log ratio R for a 5,000-point simulated dPCR experiment, each of two groups of 6,160 chambers (8 panels) where $\lambda_t = 0.24$ and $\lambda_r = 0.20$ (curve) to give a true copy ratio of 1.2, compared with the distribution of the measured log ratio for each experiment (histogram) with a mean equal to ln 1.2 and variance predicted by equation S5. (b) Observed standard deviation of $R = \ln(\lambda_t/\lambda_r)$ (points) with the theoretical standard deviation estimated using equation S5 (solid curve). Points are plotted against mean observed counts of positive observations in one panel of 770 chambers. Error bars for the points show confidence intervals for σ based on $p = 8$ observations (pairs of panels) per group, which are derived from the χ^2 distribution with $p - 1$ degrees of freedom and cover the range $(\sqrt{(p-1)s^2/\chi^2_{1-\alpha/2,p-1}}, \sqrt{(p-1)s^2/\chi^2_{\alpha/2,p-1}})$.

Power calculations

Digital PCR

We base our power calculations for digital PCR on Normal distributions. This is a reasonable approximation given the closeness of the log ratio to zero and the large number of wells. When there is no difference between target and reference, the true log ratio is zero and the *z*-statistic has a standard Normal distribution. The value of *z* is obtained as follows:

$$z = \frac{R}{\sqrt{\mathrm{var}(R)}} \tag{S6}$$

Under the null hypothesis $R = 0$, an experimental result is declared to be statistically significant, as in a *t*-test, if $z > z_0$, where z_0 is a critical value which depends on the significance level (typically 95%) and whether the test is one- or two-tailed. If the null hypothesis is not true, and in fact, say, $R > 0$, the *z*-statistic of equation S6 for this experiment is closely approximated by a shifted standard Normal distribution, centred around R/σ_R rather than zero, where $\sigma_R = \sqrt{\mathrm{var}(R)}$. A certain proportion of this distribution falls below the critical value z_0 and this defines the false negative rate β. The experimental power is defined as $1 - \beta$ and is essentially the true positive rate, that is, the proportion of results declared statistically significant when the CNV is not zero (Supplementary figure 4).

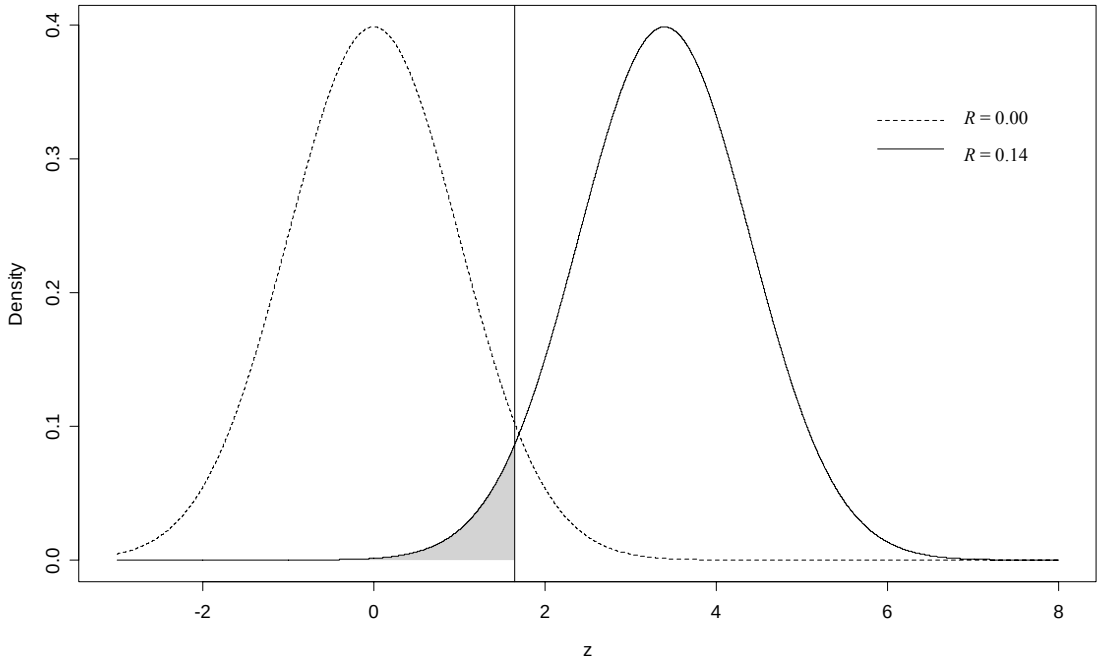

Supplementary Figure 4. Distributions of the *z*-statistic for an eight-panel experiment with $\lambda_r = 0.20$, where the CNV is 1 ($R = 0.00$; dotted line) and 1.15 ($R = 0.14$; solid line), corresponding to $\lambda_t = 0.20$ and $\lambda_t = 0.23$ respectively. The vertical line marks the critical value of *z* for a one-tailed test at a 95% significance level; the shaded area under the second distribution thus represents the false negative rate. The unshaded area is the power to detect a CNV of 1.15 with eight panels (in this case approximately 96%).

The power calculation finds the mean log ratio whose distribution of z has 5% of its area below the critical value. However, because the Normal distribution cannot be integrated with an analytical solution, this has to be done numerically. The solution proceeds as follows: if the true log ratio is R, then observed z-values are distributed as described above, and the equation to solve is

$$\frac{1}{2}\left[1+\operatorname{erf}\left(\frac{z_0 - R/\sigma_R}{\sqrt{2}}\right)\right] = \beta \qquad \text{(S7)}$$

Equation S7 can be used in a number of ways. By fixing β at, say, 5% the corresponding value of R can be found for a specific number of chambers C (σ_R depends on both R and C). Alternatively we can solve for C by setting R and finding the required σ_R, then using equation S5 to get C. The solution is usually numerical.

We used this method to generate Figure 3a in the paper. We have also produced a more general series of power curves for dPCR which can be used by a researcher to quickly determine the number of chambers required or the detectable CNV for his or her experiment without having to carry out the detailed mathematical equations described in this text. This is given in Supplementary Figure 5, and can be printed and expanded as required. For printing to large sizes, a high quality version is available from the authors on request.

Supplementary Figure 5 (on page 12). Number of chambers required to detect a specified CNV (a one-tailed test) with 95% power when λ_r is between 0.1 and 0.8. The horizontal lines correspond to the number of panels for a 48.770 digital array. Vertical lines show increments of 0.02 in the CNV to be detected.

We have also given the two-tailed equivalent (Supplementary Figure 6). This is the number of chambers required to declare the observed copy number ratio significantly different from 1. The requirement is slightly more stringent than for the one-tailed test and as such λr values for higher concentrations are given.

Supplementary Figure 6 (on page 13). Number of chambers required to detect a specified CNV (a two-tailed test) 95% power when λ_r is between 0.5 and 1.2. The horizontal lines correspond to the number of panels for a 48.770 array. Vertical lines show increments of 0.02 in the CNV to be detected.

Supplementary Figure 5 (One-tailed)

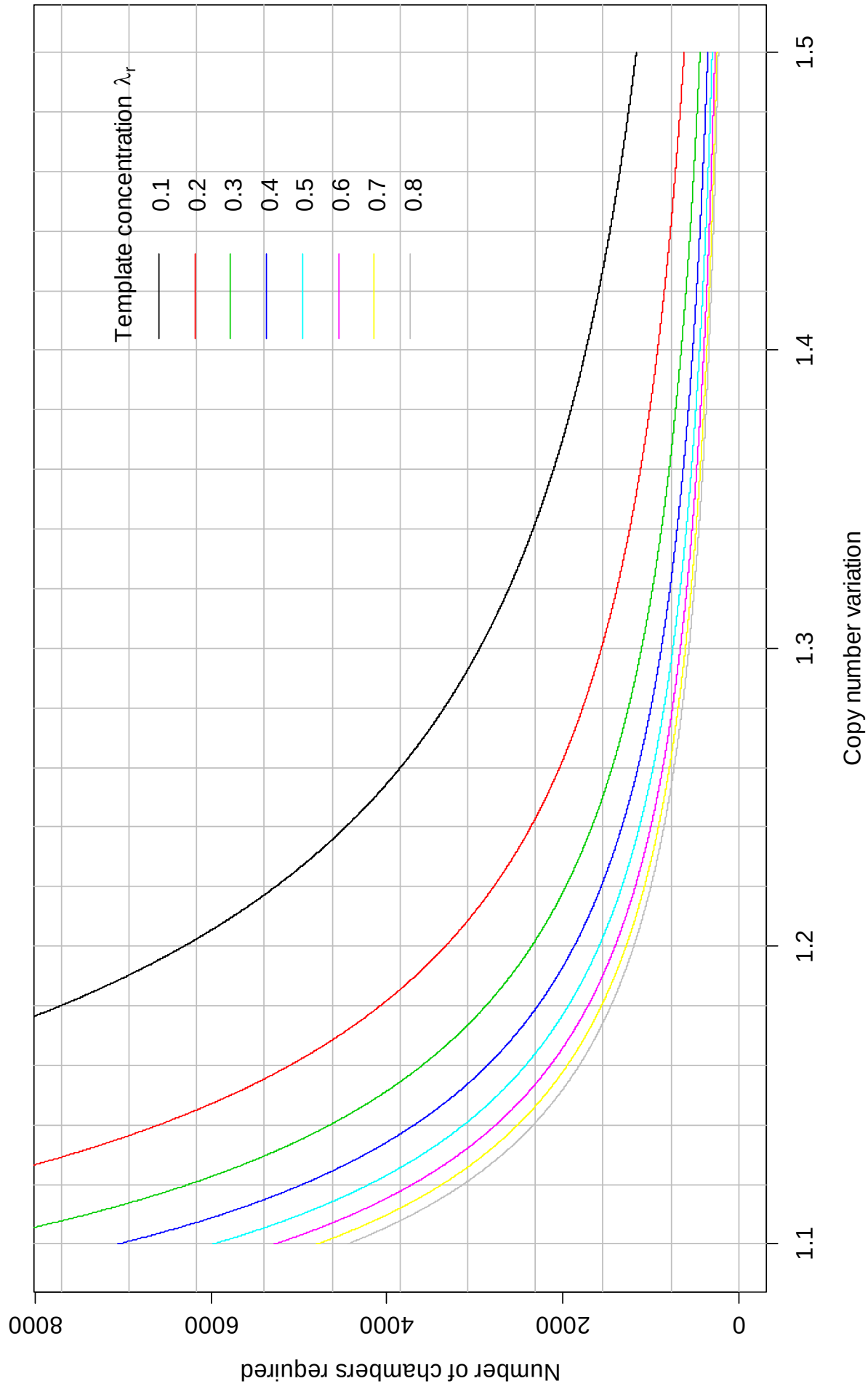

Supplementary Figure 6 (Two-tailed)

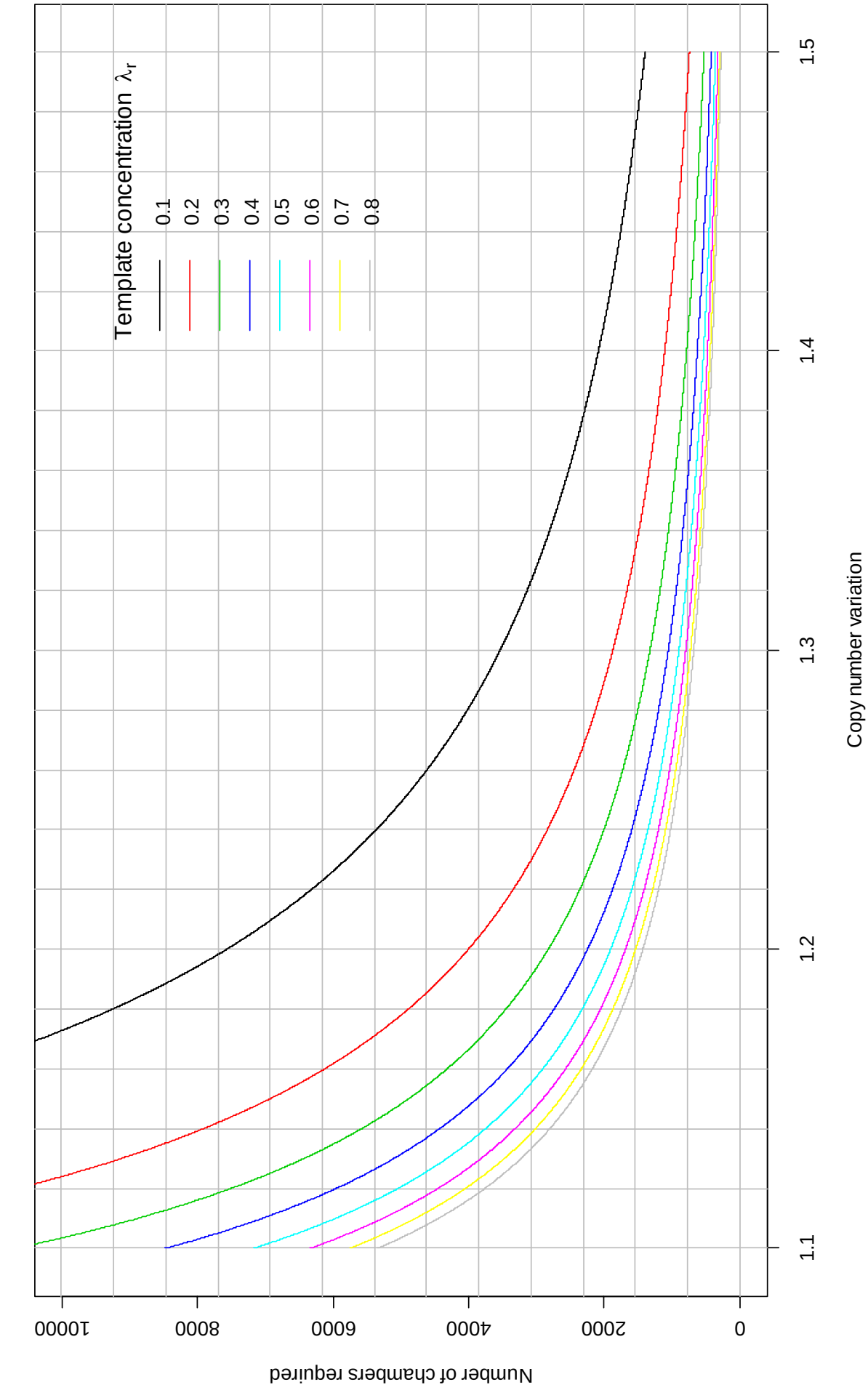

Quantitative PCR

Power calculations for qPCR were carried out using a similar principle to those for dPCR, except that the relevant statistic is the Student's *t*-statistic. The relevant test is a two-sample test using the log ratio; this tests an experimental result against a control. As for digital PCR, the log ratio is approximately Normally distributed. In this work, a result is obtained from 8 wells for the target HER2 and 8 wells for the reference RNaseP. In contrast with equation S6, the test statistic is

$$t = \frac{R_t - R_r}{\sqrt{\mathrm{var}(R_t) + \mathrm{var}(R_r)}} \tag{S8}$$

where R_t and R_r are the estimated log ratios for the target and reference respectively, and $\mathrm{var}(R_t)$ and $\mathrm{var}(R_r)$ are their variances. The variances of the two log ratios are not assumed to be the same, whether or not a pooled within-group (between-well) variance is used.

Under the null hypothesis that $R_t = R_r$, the statistic t has a Student's *t*-distribution with degrees of freedom v which can be obtained from Satterthwaite's estimate:

$$\nu \approx \frac{\left(\mathrm{var}(R_t) + \mathrm{var}(R_r)\right)^2}{\frac{\mathrm{var}(R_t)^2}{\nu_t} + \frac{\mathrm{var}(R_r)^2}{\nu_r}} \tag{S9}$$

The target and reference log ratio variances have v_t and v_r degrees of freedom respectively. Alternatively, if the variances are assumed to be equal, then the variances in R_t and R_r are calculated using pooled estimates and the *t*-value has $4(n - 1)$ degrees of freedom where n is the number of wells in each group (there are four groups: experiment target and reference, plus control target and reference). We have not assumed equal variance in our calculations, and have used the first type of test. It can be demonstrated (not shown here) that when the observed variances are similar, the two tests give very similar results.

The variance in a log ratio is obtained by error propagation, so for example the variance in the estimated log ratio for the experiment is

$$\mathrm{var}(R_t) = \frac{1}{n}\left(\frac{\mathrm{var}(c_t)}{c_t^2} + \frac{\mathrm{var}(c_r)}{c_r^2}\right) \tag{S10}$$

This has $2(n - 1)$ degrees of freedom since the estimate is obtained from two groups, each of n wells. A similar estimate is made for the reference, and the two used in equations S8 and S9 for the *t*-test.

Power calculations proceed as before except that this time, if $(R_t - R_r)$ is not zero, the *t*-statistic is distributed as a non-central *t*-distribution where the central position is the true difference divided by its standard error instead of zero. Determining n for a given value of $(R_t - R_r)$ is relatively easy to do numerically using R or some other programming language. The number of wells required to detect a log ratio which is significantly different from a control log ratio is shown in Supplementary Figure 7. To generate the power curve, the control copy numbers for the target and reference were set to 100, as was the reference copy number for the experiment. A pooled estimate of copy number standard deviation equal to 10.7 was used throughout for each group of wells, estimated from the data. Note that the standard errors required for the *t*-statistic depend on the mean copy numbers as well as the standard deviations, and so there is a relationship between the mean and variance. This is not usually the case for the Normal distribution,

and it makes the power calculation slightly less straightforward. It also means that experiments carried out with different laboratories or assays may have very different statistical power, even though the numbers of wells used is the same. Contrast this with dPCR where the variance is exactly defined in relation to the mean, and the variance in a particular dPCR experiment is fixed.

Supplementary Figure 7 indicates that a copy number ratio of between 1.25 and 1.30 can be distinguished as having a higher CNV than a control with 95% power using 8 wells per group. This fits well with our results, where a measured 1.27 was significantly higher than the Promega control, but smaller ratios were not (Figure 2b).

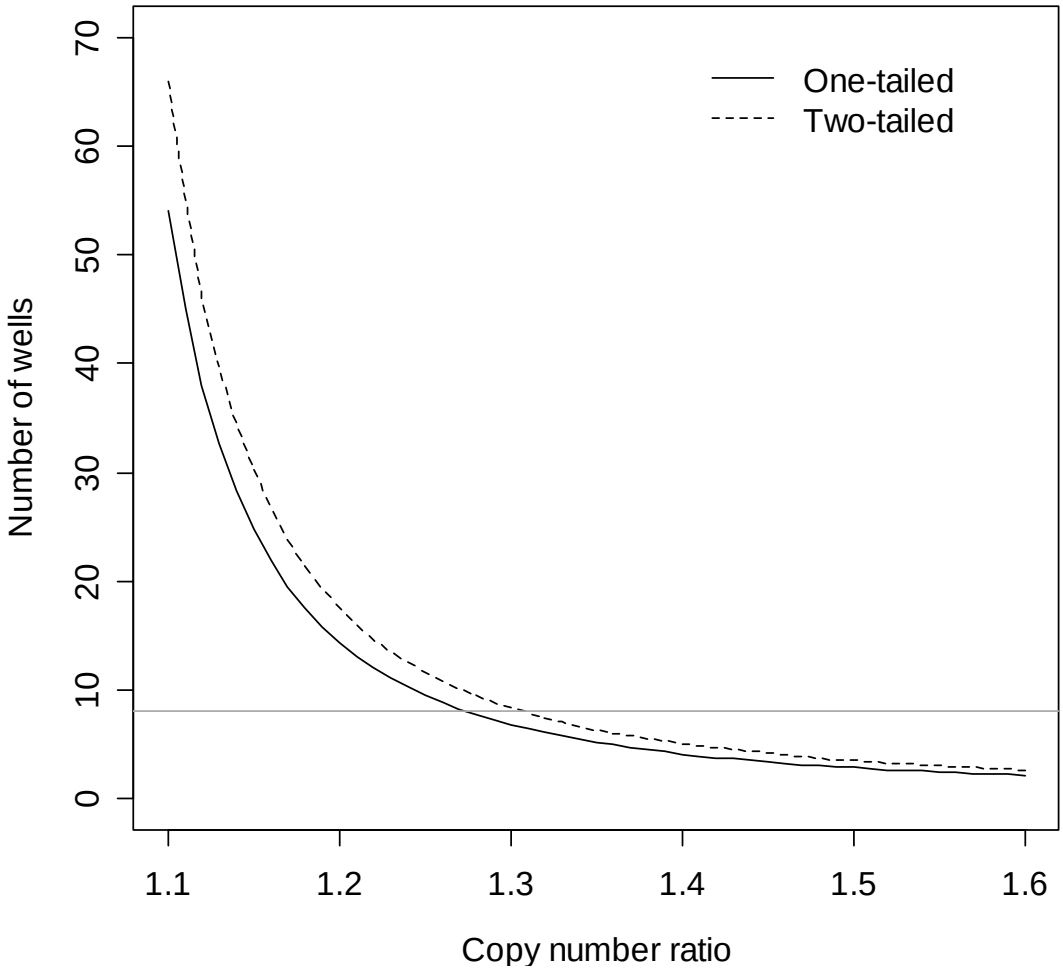

Supplementary Figure 7. Estimated number of wells per group needed to detect a given copy number ratio using qPCR, based on the results of this study. Solid line: one-tailed test (ratio significantly higher than 1); dotted line: two-tailed test (ratio significantly different from 1). The horizontal grey line represents 8 wells.